

1986

# Computer Simulation of the Hydrodynamic Lubrication in A Single Screw Compressor

W. Post

M. Swaans

Follow this and additional works at: <https://docs.lib.purdue.edu/icec>

---

Post, W. and Swaans, M., "Computer Simulation of the Hydrodynamic Lubrication in A Single Screw Compressor" (1986).  
*International Compressor Engineering Conference*. Paper 536.  
<https://docs.lib.purdue.edu/icec/536>

This document has been made available through Purdue e-Pubs, a service of the Purdue University Libraries. Please contact [epubs@purdue.edu](mailto:epubs@purdue.edu) for additional information.

Complete proceedings may be acquired in print and on CD-ROM directly from the Ray W. Herrick Laboratories at <https://engineering.purdue.edu/Herrick/Events/orderlit.html>

COMPUTER SIMULATION OF THE HYDRODYNAMIC LUBRICATION IN A SINGLE SCREW COMPRESSOR.

Dr.ir. W. Post<sup>1</sup> and Ir. M. Zwaans.<sup>2</sup>

<sup>1</sup>University of Technology, Dept. of mechanical engineering, Eindhoven, The Netherlands.

<sup>2</sup>Grasso Products B.V., Manager Research & Development, 's-Hertogenbosch, The Netherlands.

ABSTRACT.

The hydrodynamic lubrication of the teeth of the gaterotor in a single screw compressor differs from the well-known lubrication of bearings. This difference can be related to the constrained fluid film geometry and the conditions of the lubrication. Under these circumstances the convective fluid inertia will affect the performance of the lubrication. During meshing, variations of the filmgeometry and the conditions of lubrication result in variations of the distribution of the clearances. A simulation model, based on the theory of lubrication including inertial effects, has been developed to determine the periodical variations of the distribution of clearances. Changes in design can be studied and parametric analyses can be made with this model, resulting in an optimum design.

SYMBOLS.

a	Center distance.
b	Tooth-width.
e	Off center distance.
$g$	Acceleration of gravity.
h	Filmthickness.
i	Speed ratio.
$\bar{p}(\bar{x})$	Dimensionless pressure distribution.

p	Pressure.
r	Radius.
s	Clearance.
t	Time.
<u>v</u>	Velocity vector.
x	Dimensionless distance.
H	Contraction ratio.
L	Slider length.
<u>N</u>	Normal vector.
Re, Re <sup>*</sup>	Reynoldsnumber, modified Reynoldsnumber.
U	Sliding velocity.
$\alpha$	Wedge angle.
$\gamma$	Local pitch angle.
$\eta$	Dynamic viscosity.
$\theta$	Position angle.
$\rho$	Density.
$\phi$	Angle.

#### INTRODUCTION.

Most gear transmissions can be successfully utilized as rotating positive displacement machines. The single screw compressor, used in refrigeration technology, is based on the globoid wormtransmission [1], as shown in fig. 1. The performance and the reliability of this type of displacement machine is affected by the lubrication of the meshing teeth of the gaterotor. Because of the small force-density of the transmission (the gaterotors are idling) and the large relative sliding velocities the lubrication is expected to be hydrodynamic. This is in contrast to the elasto hydrodynamic lubrication of a worm power transmission. Although lubrication is hydrodynamic, it will differ from lubrication of bearings. One of these differences is the pressure difference across the teeth of the gaterotor due to the compression of the gas in

the worm grooves. Other differences are the shape of the lubrication geometry and the high sliding velocities. The general geometry of the (globoïd) screw and the gaterotor constrains the choice of the lubrication geometry, resulting in increased contraction ratios for the film. Under these circumstances the convective fluid inertia will affect the lubrication. Therefore the theory of lubrication has to be adapted to include convective fluid inertia.

In addition it is not sufficient to examine only one of the lubricated surfaces. Each meshing and lubricated flank generates a torque on the gaterotor. The combination of all torques (including the torques not resulting from lubrication) defines the position of the gaterotor in the grooves of the screw, resulting in a distribution of the clearances.

During meshing variations of the film geometries and of the conditions of lubrication, inherent to the general geometry of the single screw, will occur. Hence these variations will result in periodical variations of the distribution of the clearances. For a proper design and working conditions the periodical positions of the gaterotor should stay within the tolerances in order to avoid contact between the screw and the gaterotor. Wich would cause wear, resulting in a decrease of the capacity of the compressor and in malfunction of the lubrication.

#### GEOMETRY.

The variations of the local pitch-angles of the groove-flanks of the screw is one of the important properties of the geometry. These variations will constrain the choice of the cross-section of the teeth. The groove-flanks of the screw can be generated or manufactured in different ways, two of them will be shortly discussed.

A simple model of the generation of the groove-flanks is shown in Fig. 2. In a plane  $\pi$ , located off the centerplane of the screw, two straight and parallel lines P and S (on the pressure- and the suction-side, respectively) envelopes the groove-flanks. The Y-axis is the axis of rotation of the screw and the w-axis is the axis of rotation of the gaterotor. Rotations  $\psi$  (around the Y-axis) and  $\theta$  (around the w-axis) are coupled according:

$$\theta = i \psi \quad (1)$$

A parametric representation  $(r, \theta)$  is introduced,

whereupon the position of point G or H on the groove-flank in Fig. 2 can be represented by the vector:

$$\underline{x}_{p,s} = \begin{bmatrix} ( a - r \sin\theta \mp b \cos\theta ) \cos k\theta + e \sin k\theta \\ r \cos\theta + b \sin\theta \\ ( a - r \sin\theta \mp b \cos\theta ) \sin k\theta - e \cos k\theta \end{bmatrix} \quad (2)$$

N.B. The index p and the upper sign in  $\mp$  refer to the pressure side, the index s and the lower sign refer to the suction-side throughout this paper.

The normal  $\underline{N}$ , as shown in Fig. 3, can be derived by means of the position-vector  $\underline{x}$ :

$$\underline{N} = \frac{1}{\sqrt{m^2 k^2 + n^2}} \begin{bmatrix} m k \cos\theta \sin k\theta - n \sin k\theta \\ m k \sin k\theta \\ m k \cos\theta \sin k\theta + n \cos k\theta \end{bmatrix} \quad (3)$$

Herein:  $m = a - r \sin\theta \mp b \cos\theta$   
 $n = r - e k \cos\theta$

For the local pitch-angle  $\gamma$ , as shown in Fig.3 and defined as the angle between the normal  $\underline{N}$  on the groove-flank and the axis of rotation of the gaterotor  $w$ , the following equation can be derived:

$$\tan(\gamma)_{p,s} = \frac{i r - e \cos\theta}{a - r \sin\theta \mp b \cos\theta} \quad (4)$$

A typical example for the curves for the pitch-angle  $\gamma(r,\theta)$  is shown in the graphs of Fig. 4. These graphs clearly show the variations of the pitch-angle, especially at the outradius of the gaterotor. Consequently the normal cross-section of the teeth of the gaterotor should fit in the area bounded by the extremes of the pitch-angle, as shown in Fig.5A. This cross-section will be different for each normal section of the teeth. An obvious choice for the cross-section is one bounded by straight lines, in such way that the necessary wedges for the lubrication are formed, as shown in Fig. 5B.

The intersection of the straight lines of the cross-section forms the contactline between the groove-flank and the tooth-flank. These contactlines lie in the plane  $\pi$ . The resulting wedge-angles will depend on the coordinates  $(r, \theta)$ . During rotation the wedge-angles will vary with the tooth position angle  $\theta$ . The largest wedge-angle corresponds with the difference in the extremes of the pitch-angles in a section. From Fig. 4 can be concluded that the resulting wedge-angles are larger than the usual wedge-angles of bearings.

Another method for generating the groove-flanks is the use of a cylindrical surface instead of the straight line in Fig. 2. The same method can be used to determine the local pitch-angle and other geometric properties. A similar expression for the pitch-angle, as equation (4), can be found for this geometry. The curves of these pitch-angles differ only slightly from the curves in the graphs of Fig. 4. In order to achieve sufficient sealing it is necessary to use the same cylindrical surface for the normal cross-section of the teeth, see Fig. 5. The contact-lines between the groove-flanks and the tooth-flanks are not stationary, like the contact-lines of the straight line cross-section. Moreover these contact-lines will not lie in the plane  $\pi$ . During rotation the contactlines will roll over the tooth-flanks.

The resulting wedge geometries will depend on the coordinates  $(r, \theta)$  and will vary during rotation. The large differences in the extremes of the pitch-angles will also result in large contraction ratios (quotient of the inlet filmthickness and minimum filmthickness). Higher load capacities, due to higher accelerations of the fluid, are expected with the circular cross-section of the teeth.

#### LUBRICATION.

From the analysis of the geometry can be concluded that the resulting wedge-angles are necessarily larger than usual in bearings, resulting in greater contraction ratios for the lubricating film. In addition sliding velocities will be large. This will affect the hydrodynamic lubrication. Not only viscous effects but also inertial effects will become important. Calculations of hydrodynamic lubrication are normally based on the so-called Reynolds-equation (Reynolds 1886). This equation is obtained from the integrated forms of the continuity (5) and momentum (6) equations with all fluid-acceleration terms omitted.

$$\nabla \rho \underline{v} = 0 \quad (5)$$

$$\rho \left( \frac{\partial \underline{v}}{\partial t} + \underline{v} \cdot \nabla \underline{v} \right) = \rho \underline{g} - \nabla p + \eta \nabla^2 \underline{v} \quad (6)$$

Omission of the convective inertia term  $\underline{v} \cdot \nabla \underline{v}$  in equation (6) is based on the magnitude of the modified film Reynoldsnumber, defined as:

$$Re^* = \frac{\rho L U}{\eta} \left( \frac{h}{L} \right)^2 = Re_h \left( \frac{h}{L} \right) \quad (7)$$

where  $U$  is the slider velocity,  $h$  and  $L$  are respectively the film thickness and the length of the slider and  $\eta$  is the dynamic viscosity. Inertial effects become significant when the modified Reynoldsnumber (7) is of order or exceeds unity. This will be applicable to most of the lubrication situations in the single screw. Consequently the Reynolds equation is not suitable for this problem.

The inclusion of inertial terms in the equations of motion complicates the task of solution. The pressure field can then no longer be decoupled from the velocity field, because of the non linear inertial terms. Several methods of solution are developed, both analytical for a simplified, linearised set of equations and numerical, mostly based on solutions of boundary-layer flow [2], [3]. In this case an adapted numerical solution for flow in finite-width thrust bearings including inertial effects of Launder and Leschziner [4] is used [5].

The effects of inertial flow can be demonstrated on a steady sliding two-dimensional laminar flow. Consider the plane inclined infinite-width slider bearing of Fig. 6. The dimensionless pressure field can be obtained after considerable manipulation from the continuity and momentum equations:

$$\bar{p}(\bar{x}) = \frac{6 (H-1)(1-\bar{x}) \bar{x}}{(H+1) [1 + (H-1)(1-\bar{x})]^2} + \lambda Re^* \left\{ \ln \left( \frac{H}{[1 + (H-1)(1-\bar{x})]} \right) + \right.$$

$$- \left. \frac{\bar{x} [ 2H - (H-1) \bar{x} ] \ln(H)}{(H+1) [ 1 + (H-1)(1-\bar{x}) ]^2} \right\} \quad (8)$$

The first term of the righthand side of equation (8) is the well-known non-inertial expression for the pressure field. In Fig. 7 the dimensionless pressure distribution is shown for two different contraction ratios,  $H = 2$  for the usual bearing geometry and  $H = 12$  for the typical single screw geometry. From this figure can be concluded that inertia will have only slight effect on the usual bearing geometry. The single screw geometry, however, is strongly affected by the fluid inertia. For higher modified Reynoldsnumbers the load capacity at higher contraction ratios is expected to be much higher than the prediction of the non-inertial theory.

Experimental measurements of the pressure distribution and of the load capacity of plane inclined sliders at high contraction ratios showed good agreement with theoretical results [5].

#### SIMULATION MODEL.

The numerical model for the lubrication including inertial effects is one of the important elements of the simulation model. In this model simultaneous calculations of the lubrication of the tooth-flanks are proceeding. These calculations are not so straightforward as for single bearing geometries like the plane inclined slider. Commonly dimensions of a loaded slider are calculated for a maximum load capacity at a minimum filmthickness with respect to the working conditions (sliding velocity, viscosity of the fluid etc.) Under stationary conditions other combinations of load capacity and filmthickness may be found for such slider, i.e. load capacity and filmthickness are related:  $F = f(h)$ , see Fig. 8A.

The combined double slider, as shown in Fig. 8B, can take load in both directions or may even be unloaded. The filmthickness  $h_1$  and  $h_2$  will be adjusted depending on the difference in contraction ratios of the sliders and on the load. To determine the position of the slider ( $h_1$  or  $h_2$ ) at any load both functions  $F_1(h_1)$  and  $F_2(h_2)$  should be determined. For simple problems these functions may be expressed analitical, so the inverse function can be determined, but this is not possible for lubrication including inertial effects. In such cases the position of the slider must be determined iteratively.



The combination of sliders is not restricted to the combination of two sliders. In the simulation model all sliding surfaces of the meshing teeth are combined. Because of the radial position of the sliding surfaces torque and oblique angle  $\theta_s$  are used instead of force and filmthickness, see Fig. 9. Depending on the working conditions of the compressor, pressure in every groove is calculated. In this model, account is taken for the torques acting on the gaterotor, such as torque due to the pressure of the gas, torque of the bearings and viscous torques. The resulting oblique angle and the filmthicknesses are determined iteratively, then they are compared to the permissible values.

Because geometry is varying during rotation, calculations for the resulting oblique angle should be repeated. But these variations in geometry are periodical. So calculations need not be performed over a whole revolution of the gaterotor, but only over the cyclus angle. This angle is equal to  $2\pi$  divided by the number of teeth of the gaterotor. The purpose of the simulation model is to determine the resulting oblique angles over the cyclus angle with respect to a number of parameters. These parameters are, for example, the dimensions of the screw and the gaterotor, the number of revolutions per minute, the viscosity and the density of the lubricating fluid, the values and the distribution of the clearances and the working conditions of the compressor.

## RESULTS.

With the aid of the simulation model variations of the resulting oblique angle have been calculated for a range of single screw compressors with both the straight line cross-section and the circular cross-section of the teeth. The effects of the values and the distribution of the clearances as well as the effects of the working conditions of the compressor have been examined. In the graph of Fig. 9 a typical example of the variations of the resulting oblique angle is shown. Permissible values for the oblique angle (to prevent metallic contact between gaterotor and screw) are also indicated in this graph. The curve of the resulting oblique angle will shift towards the permissible value (towards the line of metallic contact) when the pressure difference of the compressor is increased. So working conditions of the compressor are restricted by the lubrication.

In general it was found that the performance of the circular cross-section was much better than the performance of the straight line cross-section. This can

also concluded from the graphs in Fig. 10. These graphs show the resulting torque and the resulting filmstiffness versus the oblique angle for the two cross-sections at a certain value of the cyclus angle.

#### CONCLUSION.

A simulation model has been presented for determining the periodical variations of the resulting oblique angle (or the filmthicknesses) of the meshing teeth in a single screw compressor. This model is based on a lubrication theory including inertial effects. It was shown that inertia effects will play an important rôle in the lubrication of the single screw. Changes in the values and distribution of the clearances as well as changes in the working conditions of the compressor have been examined for two different cross-sections of the teeth. It was found that the teeth with the circular cross-section performed better than the teeth with the straight line cross-section. Further changes in design can be studied and parametric analyses can be made with this simulation model, to optimize the lubrication of the single screw.

#### REFERENCES.

- [1] Reuleaux, F und Moll, C.L. Der Constructeur, IV Auflage (1882-1889)
- [2] Saibel, E.A. and Macken, N.A. "Nonlinear Behavior in Bearing: A Critical Review of Literature." ASME Journ. of Lub. Techn., Vol 96, No. 1, 1974, pp174-181
- [3] Milne, A. "Inertia Effects in selfacting Bearing Lubrication Theory." Int. Symp. on Lub. and Wear 1963, Houston, McCutchan Pub. Co., pp429
- [4] Launder, B.E. and Leschziner, M.A. "Flow in Finite-width Thrust Bearing including Inertial effects. 1-Laminar Flow." ASME Journ. of Lub. Techn., Vol 100, July 1978, pp330-338
- [5] Post, W.J.A.E.M. "De hydrodynamische filmsmering in een globoïde wormcompressor." PhD Thesis, University of Technology Eindhoven, 1983

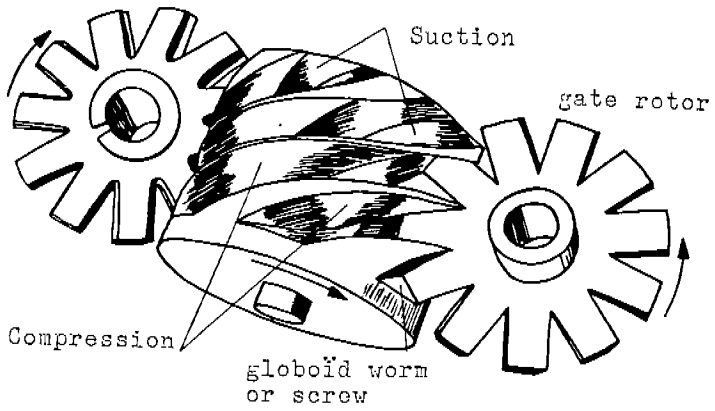


Fig. 1. The single screw compressor.

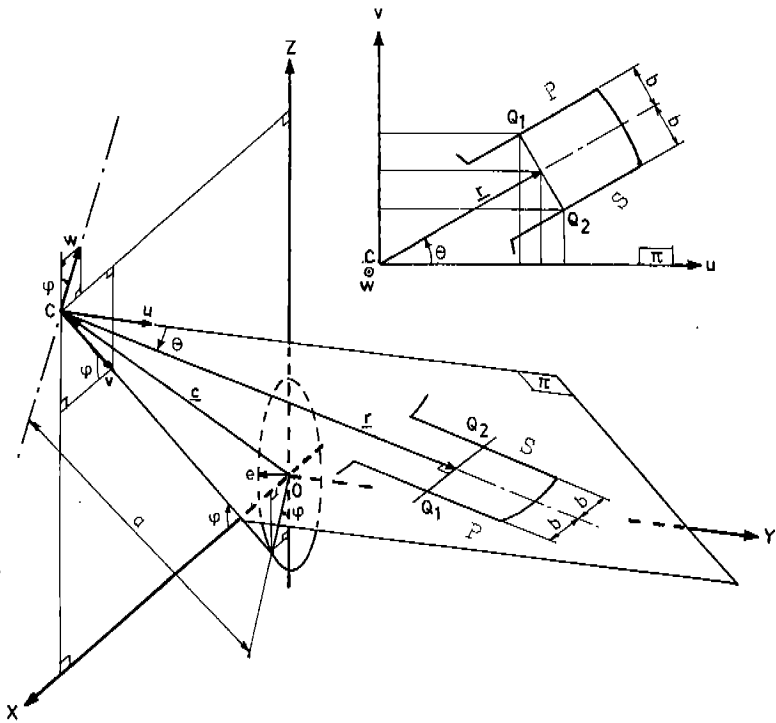


Fig. 2. The generation of the groove-flanks.

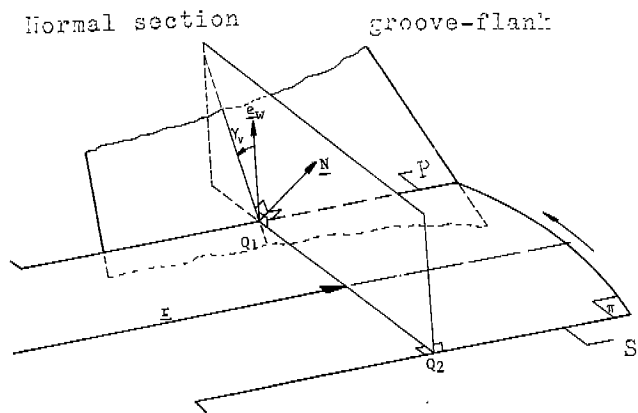


Fig. 3. The local pitch-angle.

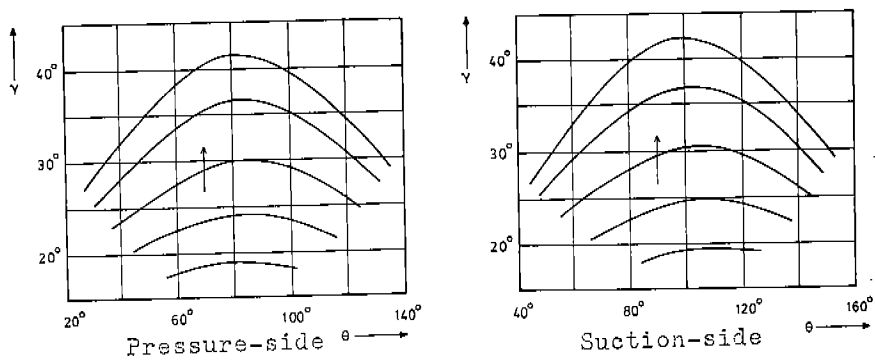
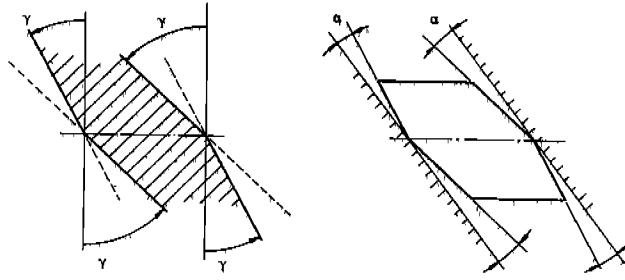
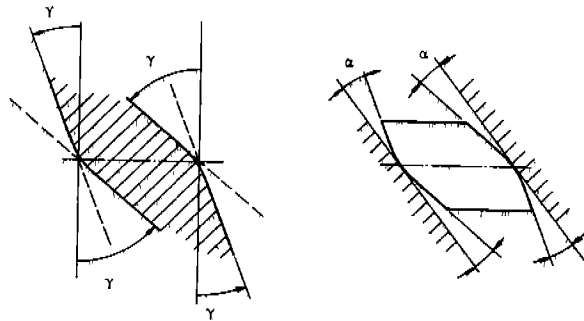


Fig. 4. The distribution of the local pitch-angles.



Straight line cross-section



Circular cross-section

Fig. 5. The tooth-profiles.

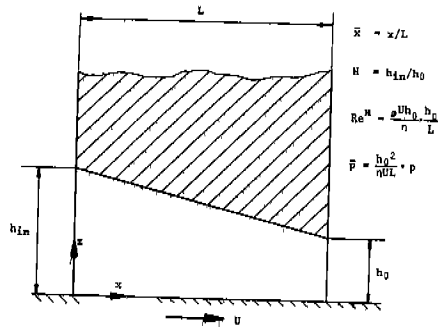


Fig. 6. The plane inclined infinite-width slider.

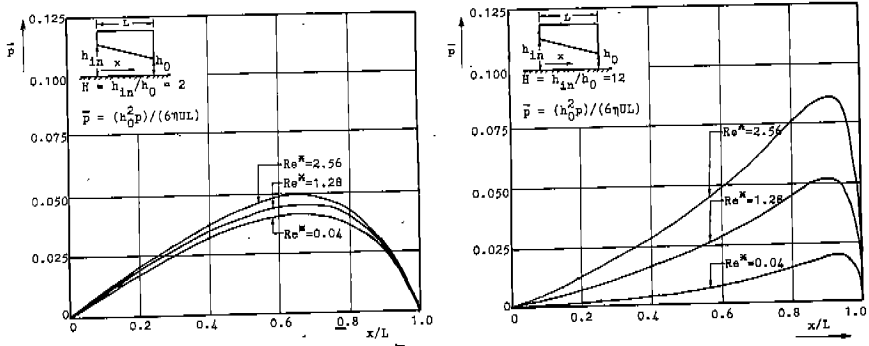
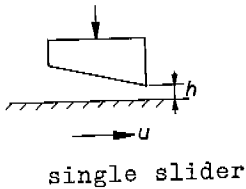
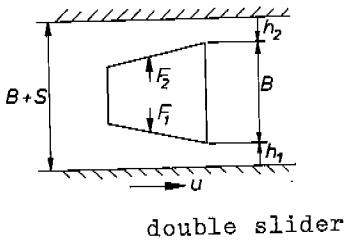
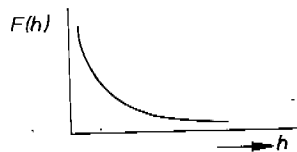


Fig. 7. Nondimensional pressure distribution of the slider.



single slider



double slider

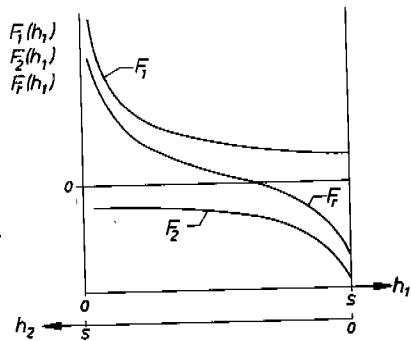


Fig. 8. Load capacity versus minimum film thickness.

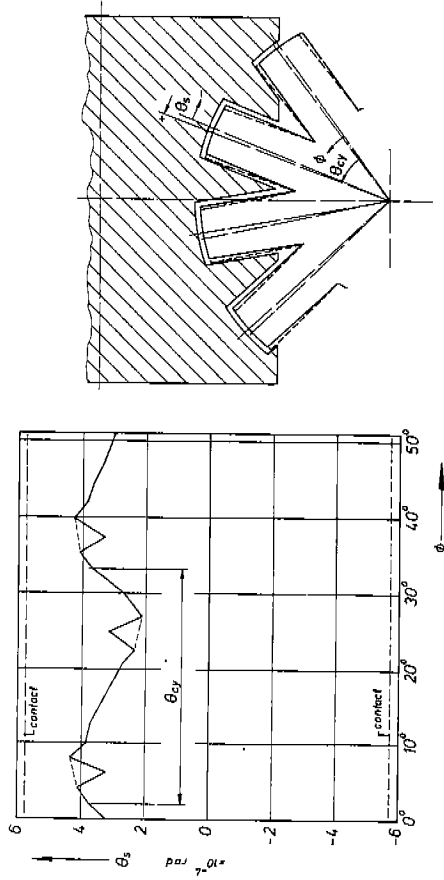


FIG. 7. Variations in resulting oblique-angle.

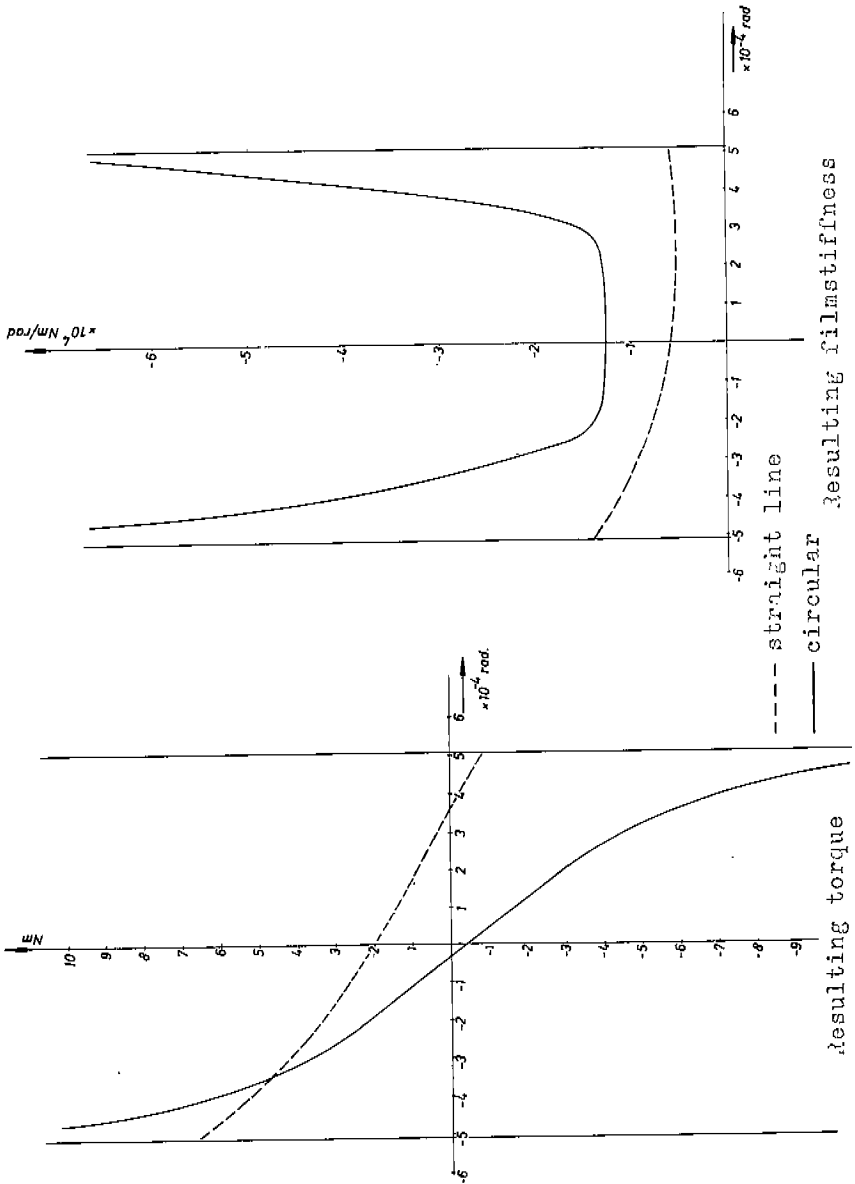


Fig. 10. Resulting torque and filmstiffness versus oblique-angle.



THE COMPUTER SIMULATION OF OIL-FLOODED REFRIGERATION TWIN-SCREW COMPRESSORS

Dagang Xiao, Zenan Xiong and Yongzhang Yu

Chemical Machinery & Equipment Division, Xi'an Jiaotong University, Xi'an, Shaanxi, China

James F. Hamilton

Ray W. Herrick Labs. , Purdue University, U. S. A.

ABSTRACT

A mathematical model considering the effect of real gases is developed to predict the effect of some actual factors, such as gas leakage, heat exchange between gas and flooded oil, and flow resistance at discharge port, etc. , on the performance of oil-flooded twin-screw compressors. A prediction program has been written to be available to ammonia and 12 kinds of freons including R22, R12, R502, etc. . The analytical formulas of geometrical characteristics such as control volume, sealing line length and discharge port area, etc. , for the sample profile are obtained. Some calculated results of P-V diagram, volumetric efficiency and adiabatic efficiency are enumerated in this paper.

NOMENCLATURE

- A area; centre distance between male and female rotors
- $C_l$  specific heat of liquid (oil)
- $C_v$  vapor specific heat at constant volume
- $D_o$  nominal diameter
- E mechanical energy
- h specific enthalpy
- i transmission ratio
- k ratio of  $C_p$  to  $C_v$